

Research on Fluid Suspension and Its Stability

Liu Kaiming, Zhou Yajie, Zhao Shumin, Wang Hongli

(School of Physics, Xi'an Jiaotong University, Xi'an, Shaanxi 710049)

Abstract : The phenomenon of the suspension of cylinders and spheres in the jet column is studied. The N-S equation and boundary layer theory are used to establish a model for the flow around the side of the cylinder. The numerical calculation method solves the velocity field of the water flow and the air flow, solves the pressure gradient force and viscous moment, establishes the equilibrium equation to solve the stable suspension of the object Altitude and steady-state rotational speed. The results show that the suspended height and steady-state rotational speed of the object are approximately quadratic functions with the diameter of the cylinder. through control variables method to explore the stability of suspended objects, and found that it is affected by multiple factors such as the thickness, diameter and shape of the object.

Key words: lightweight object; free jet column; suspended height; steady-state rotational speed; stability

CLC number: O351.2 **Document identification code:** A **DOI:** 10.19655/j. cnki. 1005-4642.2021.03.010

Lightweight objects can be ejected at the edge of the free jet column part is in stable suspension and starts while levitating. Rotation, this phenomenon is called fluid suspension. Suspension of an object in a fluid Floatation is an emerging physical problem that has attracted much attention at present. This topic involves related research on the frontiers of fluid mechanics, such as Navier-Stokes equation, boundary layer theory, etc. Fluid suspension applications are also Very extensive, such as China's domestic liquid suspension non-energy rod control in the nuclear field control system [1] and the more mature liquid suspension passive in the world Shutdown system [2], liquid suspension permanent magnet multi-freedom in modern industry degree motor, and so on.

1 Fluid suspension model

1.1 Experimental setup

The water supply system is composed of a faucet and a hose, and the hose is discharged. The end is fixed, and the fixing device is made of 2 identical iron triangles and iron rods. For support, fix the water outlet with a rotatable cross clip, which is supported by magnets and The iron block is used as the stabilizer of the cross clip, so that the angle of the water spray is fixed.

1.2 Experimental phenomenon

In the experiment, the cylinder is placed statically on the edge of the free jet, Within 1 s after the hand is released, the cylinder will start to rotate, and the height tends to be fixed. fixed value, the speed remains basically constant.

1.3 Model construction and theoretical analysis

The suspension model is shown in Figure 1, where is G for cylinder weight force, F_1 the water flow impulse, F_2 is the pressure gradient force, M_1 for water flow

viscous moment, M_f is the air viscous moment.

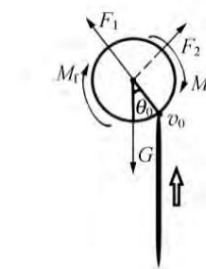


Figure 1. The suspension model of the cylinder

When the cylinder is suspended, it vibrates slightly up and down around the equilibrium point. The amplitude is approximately constant, and this point is defined as the stable suspension of the light object height, at this time the cylinder is force balanced:

$$F_1 + F_2 + G = 0,$$

The steady-state rotational speed of the cylinder is approximately constant, and the resultant moment received by the cylinder

$$M_1 + M_2 + M_f = 0,$$

when no object is suspended, the height of the water column is h_0 . Water spray quality per second is, then initial rate of water flow is b , the water flow rate at the suspension height is 0, because objects that are too light cannot be suspended, while objects that are slightly heavier The suspension height is low, so the and in the experiment are more connected v_0 . It can be approximated that the radius of the water column is equal to the radius of the water pipe R_1 , at the moment when the water column hits the side of the cylinder, its momentum can be Divided into the radial and normal directions along the cross section of the cylinder, where along the cylinder The impulse in the radial direction of the body is all converted into the impact force on the cylinder F_1 ,

Received date: 2020-08-27; Modified date: 2020-10-14

About the author: Liu Kaiming (2002-), male, born in Xi'an, Shaanxi Province, undergraduate student of the 2019 grade in the School of Physics, Xi'an Jiaotong University.

Corresponding author: Zhao Shumin (1977-), female, from Xi'an, Shaanxi Province, associate professor at the School of Physics, Xi'an Jiaotong University, Ph.D., research direction is condensed matter

Physics, Biophysics. E-mail: zhaosm@xjtu.edu.cn

Wang Hongli (1964-), male, born in Xi'an, Shaanxi Province, professor of the School of Physics, Xi'an Jiaotong University, Ph.D.

Semiconductor Physics. E-mail: hlwyxs@mail.xjtu.edu.cn



Its size is the angle $\rho_0 \cos \gamma_0$, γ_0 is the center point of the impact surface and the cylinder between the line connecting the axis and the vertical direction, which is called the eccentric angle.

$$F_1 = S p \cos \gamma_0, \quad (3)$$

Will p_0 and S Substituting the expression into (3), we get:

$$F_1 = 2 \gamma_0 \omega^2 R^2 \cos \gamma_0 \sqrt{h_0 - h} h_0, \quad (4)$$

(where is the fluid resistance of the cylinder to the Coanda

The surface forms a flow around the surface, and the flow around the surface is due to viscous resistance in the upward process.

and the rate of gravitational action will gradually decay, the width will increase, and the thickness will gradually increase.

Thinning, after bypassing the highest point, the speed gradually increases, the width increases,

The thickness continues to thin, forming a flow around.

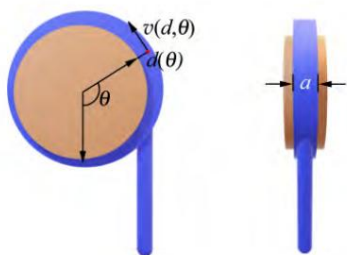
First solve the two-dimensional velocity distribution (the flow range around the plane is not regular ring), due to the lateral symmetry of the cylinder, it can be close to

It seems to be considered that the windings at the same height, the same angle, and the same thickness

The flow rates are equal, so the two-dimensional model can be extended to three-dimensional.

Assume that the range of the coverage angle of the surrounding flow is 2γ , and the width is

time, it is regarded as a steady flow, any fluid element is taken, its location (d, θ) , as shown in Figure 2, speed is $v(d, \theta)$,



(a) side view (b) top view

Figure 2 Suspension of the cylinder

When the whole system reaches a steady state, any position on the side of the cylinder

The velocity of the fluid element at the location and the thickness of the surrounding flow do not change with time

The flow system is described by the N-S equation:

$$\frac{V}{dt} = -1 \frac{\partial \gamma}{\partial t} p + \gamma^2 V, \quad (5)$$

Simultaneous continuity equations:

$$\frac{1}{r} \frac{\partial \gamma}{\partial r} (rVr) + 1 \frac{\partial \gamma V \gamma}{\partial \gamma} + \gamma \frac{\partial V}{\partial z} = 0.$$

The boundary layer theory [1] is introduced to describe the flow system without considering the external

Layer viscous resistance and no-slip condition, the N-S equation can be simplified as

$$\begin{aligned} \gamma \left(\frac{\partial V}{\partial t} + V_r \frac{\partial V}{\partial r} + \frac{\partial \gamma}{\partial \gamma} \frac{\partial V}{\partial \gamma} + \frac{V}{r} \frac{\partial^2 \gamma}{\partial \gamma^2} \right) &= -1 \frac{\partial p}{\partial r}, \\ \gamma \left(\frac{\partial V \gamma}{\partial t} + V_r \frac{\partial V \gamma}{\partial r} + \frac{\partial \gamma}{\partial \gamma} \frac{\partial V \gamma}{\partial \gamma} + \frac{V}{r} \frac{\partial V \gamma}{\partial \gamma} \right) &= -1 \frac{\partial p \gamma}{\partial \gamma}, \\ \frac{1}{r} \frac{\partial \gamma}{\partial r} (rVr) + 1 \frac{\partial \gamma V \gamma}{\partial \gamma} &= 0. \end{aligned}$$

Use the finite difference method to obtain the numerical solution of the system of differential equations,

The time step is 0.1 s, the space step is 10^{-5} m, and the angle step is

Take $2\gamma/100$, and iterate over time after confirming the initial conditions. when

The iteration is stopped when the data difference between two adjacent generations is less than 1%.

For the flow in the boundary layer, the value of the Reynolds number [2] is

$$Re = \frac{\gamma V L}{\mu} \approx 1 \times 10^5 < 5 \times 10^5,$$

In the γ is the water flow density, taken as 103 kg/m^3 ; is the V is the flow velocity,

V formula, $< 10 \text{ m/s}$ L characteristic length, here refers to the diameter of the cylinder, L

s; in the order of 10^{-2} m ; is the dynamic viscosity of water, which is taken at 20°C

$1.01 \times 10^{-3} \text{ Pa}\cdot\text{m}$. Since the Reynolds number is less than 5×10^5 , then

The flow in the boundary layer can be analyzed as laminar flow, which means

boundary layer thickness, the velocity at can be written as

$$\frac{V(y)}{V_0} = f\left(\frac{y}{\delta}\right),$$

Taylor expansion and taking the first-order approximation, we get:

$$V(y) = a_0 V.$$

Combining the flow around the boundary layer with the velocity distribution around the outer layer, we get

The complete flow velocity field around the lateral flow is shown in Fig.3.

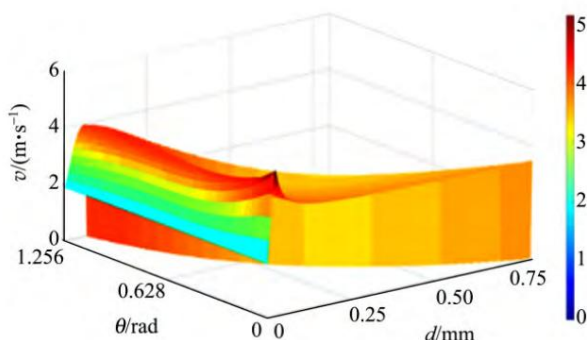


Figure 3 Velocity field of water flow around

In Figure 3, the flow velocity of the first layer close to the side of the cylinder decreases

Not obvious, but the thickness of the water film becomes thinner as the cylinder rotates, and the momentum and

The transfer of energy is reflected in the loss of the thickness of the water flow layer, which is

The momentum and energy of the split water become the angular momentum and energy of the cylinder's rotation

quantity. The pressure distribution is solved by the flow velocity field, and the pressure in the boundary layer is

There is a gradient perpendicular to the wall direction, which satisfies the momentum integral equation [3]:

$$\frac{d}{dx} (U t^2) + d \frac{U}{dx} U \gamma = \frac{\partial \gamma}{\partial \gamma},$$

Using the Thwaites solution method [1] to solve, the momentum thickness is t , but

$$t^2 = \frac{0.456 v}{U(x \gamma)} \int_0^x U^5 d \gamma,$$

$U(x)$ is the flow velocity distribution around the flow, through the previous finite difference method, namely

Can be solved. Define momentum thickness of dimension 1

$$K = \frac{t^2}{v} \frac{dU}{dx},$$

Combining flow velocity distribution and momentum thickness to solve the viscosity of each fluid element

Stress distribution

$$\ddot{y}_0 = \frac{\ddot{y}U}{t} (K + 0.09) 0.62,$$

Summing up all the fluid elements in direct contact with the cylinder, we get

The viscous moment is

$$M_1 = \ddot{y} \sum_1^N \ddot{y}_0 (\ddot{y} r a \ddot{y} \ddot{y}). \tag{6}$$

When the boundary layer is very thin, the flow perpendicular to the solid boundary can be ignored speed, then the N-S equation in the boundary layer can be simplified as

$$\frac{\ddot{y} p}{\ddot{y} r} = \frac{\ddot{y} V}{r} \ddot{y}^2 - 2 \frac{\ddot{y}}{r^2} \frac{\ddot{y}_v \ddot{y}}{\ddot{y}}, \tag{7}$$

The pressure distribution on the side of the cylinder can be obtained * (and consider the flow around the

Gravity force), summing all the elements to get the pressure gradient force as

$$F_2 = \ddot{y} \sum_1^N [p(\ddot{y}) - \ddot{y} g z(\ddot{y})] r a \ddot{y} \ddot{y}, \tag{8}$$

The air velocity field can be obtained by solving the water velocity field.

Figure 4 shows the change trend of the air velocity field within 5 minutes. The gas viscous moment is on the order of 10-9 N m, the moment of inertia of the cylinder In the order of 10-5kg·m2 , the air viscous moment can be ignored.

The balance equation can be written as:

$$F_1 + F_2 + G = 0,$$
$$M_1 = \ddot{y} \sum_1^N \ddot{y}_0 (\ddot{y}) r a \ddot{y} \ddot{y} = 0. \tag{9}$$

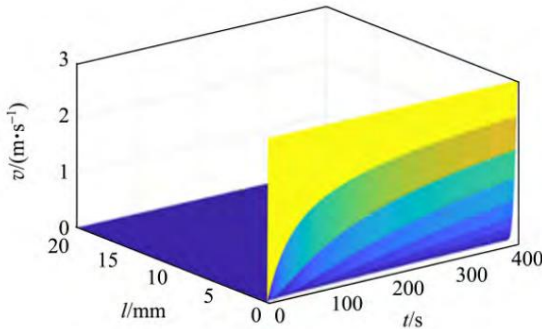


Figure 4 Air velocity field

1.4 Numerical simulation

Set the initial array (h) to be (0, 0), respectively 0.1r/s and 0.01m as the step size increase (Δh), find out the corresponding The flow velocity field of , find the resultant force and resultant moment, take the An array close to 0, at this time (Δ) is the reason for the given cylinder

The desired rotational speed and the ideal suspension height are shown in Figure 5. Initial conditions: Height 3cm, diameter 12cm, mass 4.63g, initial height of water column Set to 1.60 m. Numerical simulation results: The theoretical speed is 5.33r/s, the theoretical suspension height is 1.09m.

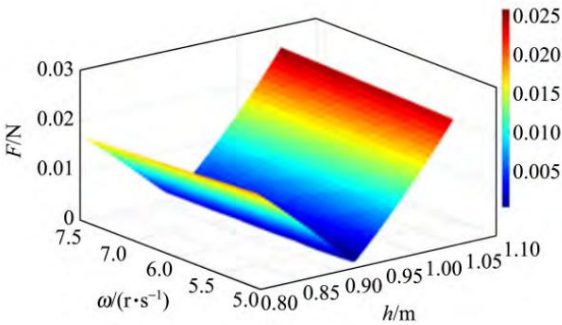


Figure 5 Theoretical steady-state speed and suspension height

2 Determination of suspension height and rotational speed

Use Tracker software to measure the steady-state suspended height and steady-state rotational speed h_e of the cylinder, and obtain the relationship with the diameter and thickness of the cylinder. D

relationship with the theoretical suspension height t, the theoretical steady-state speed

ω_t Compared.

2.1 ω relationship with

The experimental results show l As shown in Table 1 and Figure 6, and " < 0, l a quadratic function, the coefficient of the quadratic term is less than 0, and the ω the real experimental curve is in good agreement with the theoretical curve.

Table 1 ω , h and l The data

D/cm	l/cm	ω/(r·s-1)		h/m	
		theoretical	experiment	theoretical	experiment
11.81	2.02	5.33	4.71	1.25	1.05
11.82	3.02	6.31	5.05	1.09	0.89
11.79	4.00	7.05	5.86	0.95	0.75
11.83	5.01	7.48	6.13	0.85	0.67
11.80	6.03	7.55	6.46	0.78	0.61

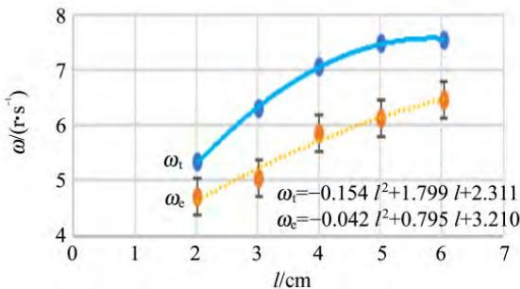


Figure 6 Speed ω and thickness l Relationship

2.2 ω and D Relationship

experimentally measured and D As shown in Table 2 and Figure ω_t and D The relationship is quadratic function, the coefficient of quadratic term is greater than 0, and ω_t " > 0, the real the empirical curve is in good agreement with the theoretical curve.

Table 2 \bar{y} and h and D data

D /cm	l /cm	$\bar{y} /(\text{r}\cdot\text{s}^{-1})$		h /m	
		theoretical	experiment	theoretical	experiment
5.91	3.02	5.25	4.31	1.51	1.34
7.94	3.01	5.40	4.68	1.32	1.19
9.98	3.03	5.76	4.80	1.18	1.06
11.82	3.02	6.31	5.05	1.08	0.89
14.87	3.00	7.67	5.72	0.99	0.83

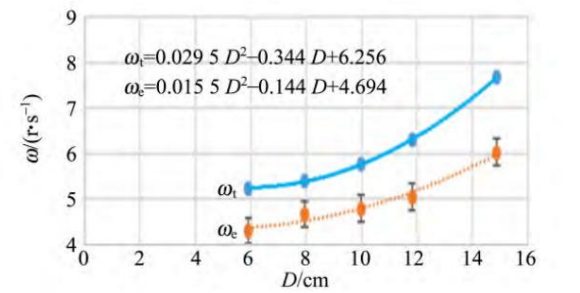


Figure 7 Speed \bar{y} and diameter D Relationship

2.3 h relationship with

experimentally measured with h . As shown in Table 1 and Figure 8, h and l are both quadratic functions. The relationship is quadratic function, the coefficient of quadratic term is greater than 0, and h is the real quantity. The empirical curve is in good agreement with the theoretical curve.

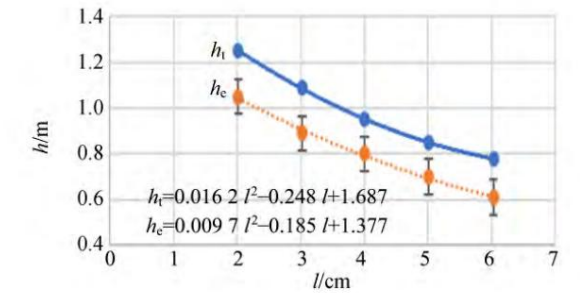


Figure 8 Suspension height h and thickness l Relationship

2.4 h D Relationship

and the experimental results are shown in Table 2 and Figure 9. h is in a quadratic function relationship with the quadratic term coefficient greater than 0, and h is greater than 0, the experimental curve is in good agreement with the theoretical curve.

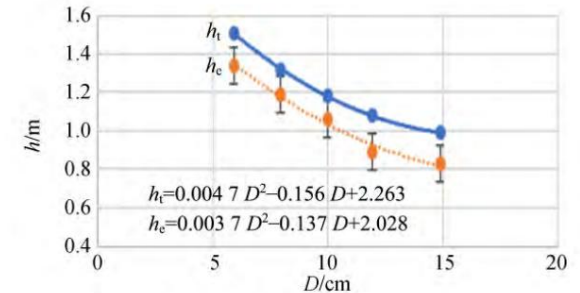


Figure 9 Suspension height h and diameter D Relationship

3 Stability of fluid suspension

3.1 Experimental investigation of stability

Stability of Suspended Objects and Stabilization of Ecosystem Resistance

Sexuality and resilience stability characteristics are well matched, both with their own structure.

The structural characteristics are related to the intensity of external interference [7], so the introduction of biological

The concept of science, to explore the resistance and resilience stability of suspended matter.

3.1.1 Resistance stability

Suspended objects are continuously disturbed and their intensity increases, causing

The maximum disturbance intensity that it can withstand is used as a measure of resistance stability

the standard. The initial height of the water column is h , the mass of suspended objects, slowly

Slowly change the angle between the water column and the \bar{y} found, as the water column and the vertical direction

The included angle increases, and the intensity of the disturbance also increases gradually, when the water column is

When the included angle in the vertical direction increases to a certain value, the object just reaches

When the balance limit falls, immediately stop changing the water column and the vertical direction.

The included angle, the relationship between the horizontal distance \bar{y} and \bar{y} of the measured jet ejection x, \bar{y}, x

point and \bar{y} the landing point is:

$$\cos(\bar{y} - \bar{y}) = \frac{x}{4h_0}.$$

\bar{y}, x The larger the \bar{y} value is, the greater the \bar{y} is, and the stronger the resistance stability is. In the x

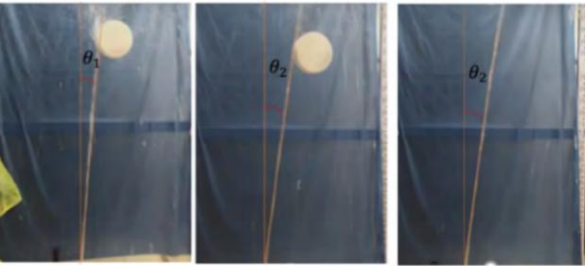
experiment, the arithmetic mean \bar{y} of \bar{y} is taken as the standard to measure the resistance stability.

1) Cylinder

Figure 10 shows the process of the cylinder from stable suspension to equilibrium limit.

The experimental measurement of \bar{y} and, as shown in Table 3 and Figure 11, the cylinder

The resistance stability is the strongest at = 3.02cm.



(a) increase the exit angle (b) critical angle (c) drop

Figure 10 Changing the exit angle (cylinder)

Table 3 \bar{y} and \bar{y}_s and l Relationship

D /cm	l /cm	\bar{y}_x /cm	\bar{y}_s /(°)
11.81	2.02	43.3	12.5
11.81	3.02	67.6	18.3
11.79	4.00	49.5	15.4
11.83	5.01	35.3	10.6
11.80	6.03	27.3	9.4

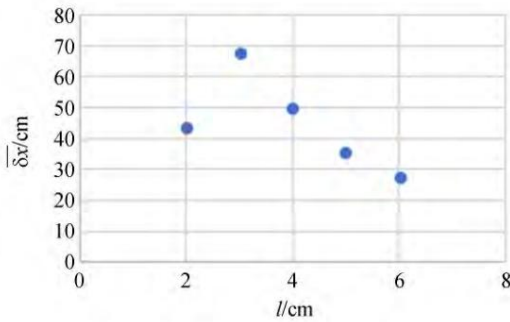


Figure 11 $\bar{\Delta x}$ and l Relationship

Experimentally measured $\bar{\Delta x}$ and l , as shown in Table 4 and Figure 12, the cylindrical delta and body resistance stability at $l = 11.81\text{cm}$ when the strongest.

Table 4 $\bar{\Delta x}$ and $\bar{\Delta s}$ with l data (cylinder)			
l/cm	l/cm	$\bar{\Delta x}/\text{cm}$	$\bar{\Delta s}/(^{\circ})$
5.91	3.02	15.4	5.1
7.94	3.01	24.6	11.2
9.98	3.03	42.3	14.5
11.81	3.02	67.6	18.3
14.87	3.00	40.5	13.6

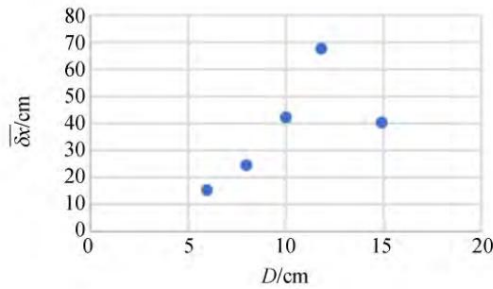
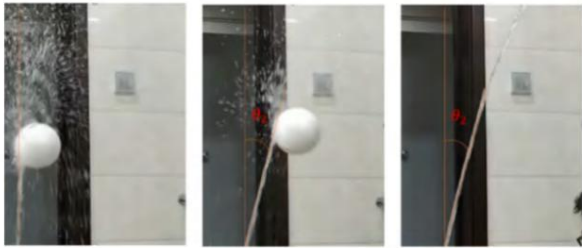


Figure 12 $\bar{\Delta x}$ and l Relationship of (Cylinder)

2) Sphere

The resistance stability experiment of the ball is shown in Fig. $\bar{\Delta x}$ and l as shown in Table 5 and Figure 14, the resistance stability of the sphere exist $l = 14.37\text{cm}$ when the strongest.



(a) increase the exit angle (b) critical angle (c) drop

Figure 13 Changing the exit angle (sphere)

Table 5 $\bar{\Delta x}$ and $\bar{\Delta s}$ with l data (sphere)

l/cm	$\bar{\Delta x}/\text{cm}$	$\bar{\Delta s}/(^{\circ})$
4.74	9.3	10.7
5.76	22.4	14.0
9.80	58.1	26.3
11.80	75.8	33.6
14.37	100.3	50.4
18.55	64.2	41.1

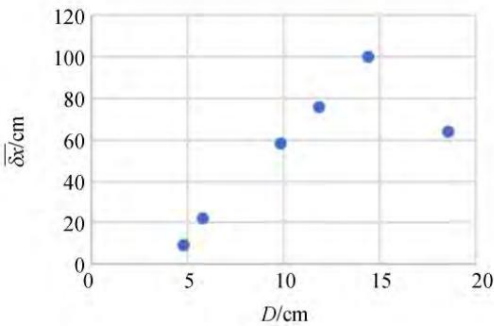


Figure 14 $\bar{\Delta x}$ and l relation (sphere)

3.1.2 Restorative force stability

The suspended matter can return to the suspended state after instantaneous disturbance. state, which is called restoring force stability. Tie the weights with a thin, lightweight thread On the cantilever, the length of the suspension wire = 1.000m, the suspension wire and the vertical The included angle is 5° , and the static release weight hits the side of the suspended object. If the object does not fall, increase the angle s between the suspension line and the vertical direction $\bar{\Delta s}$, step With a length of 5° , the impact energy converted from the gravitational potential energy stored by the weight increases. Large, when the release angle increases to a certain value, the object will not be hit after being hit. This angle is called the critical angle, the relationship between the weight $\bar{\Delta l}$. release angle and the gravitational potential energy E_g and the impact energy E_k .

The system (ignoring the effect of air resistance) is

$$E_g = m g \sin \bar{\Delta s}, \quad E_k = \frac{1}{2} m v^2$$

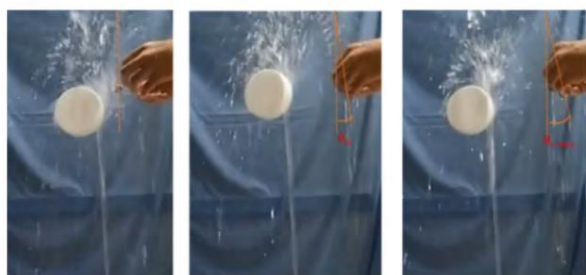
which can be approximated as a constant, which is related to the energy in the collision process loss related.

$$E_k = m g \sin \bar{\Delta s}$$

in $\bar{\Delta s} \approx \frac{\pi}{4}$, when $\bar{\Delta s} \approx \frac{\pi}{4}$, E_k and $\bar{\Delta s}$ positive correlation. In experiment Take $\bar{\Delta s}$ the arithmetic mean of $\bar{\Delta s}$ as a measure of resilience stability the standard.

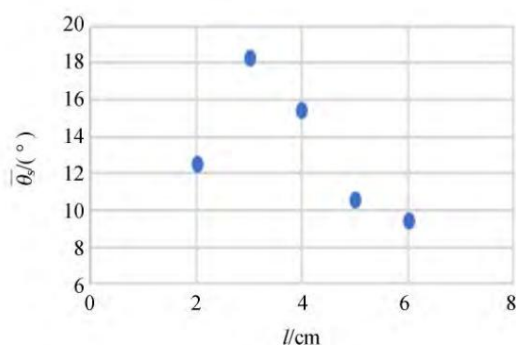
1) Cylinder

The stability of the restoring force of the cylinder is shown in Figure 15. The measured $\bar{\Delta x}$ and l As shown in Table 3 and Fig. 16, the restoring force stability of the cylinder $l = 3.02\text{cm}$ is the strongest at 3.02 cm.

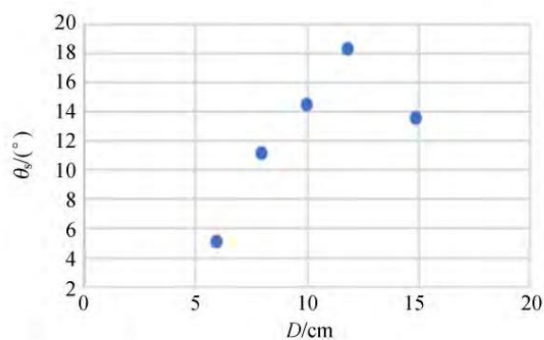


(a) at rest (b) pulling off the weight (c) critical release angle

Figure 15 Weight Impact (Cylinder)

Figure 16 $\bar{\gamma}_s$ and l Relationship

The measured $\bar{\gamma}_s$ and \bar{D} As shown in Table 4 and Figure 17, the cylinder recovers and force are stable at $\bar{D} = 11.81\text{cm}$ when the strongest.

Figure 17 $\bar{\gamma}_s$ and \bar{D} Relationship of (Cylinder)

2) Sphere

The sphere restoring force stability experiment is shown in Figure 18. $\bar{\gamma}_s$ and \bar{D} shown in Table 5 and Fig. 19, the restoring force stability of the sphere In $\bar{D} = 14.37\text{cm}$ is the strongest, and the diameter deviates from 14.37cm will the resulting decrease in stability, for spheres and cylinders of the same diameter, The restoring force of the sphere is more stable.

Comparing two kinds of stability experiments, it is found that the sphere and the cylinder

The resistance stability and resilience stability of the

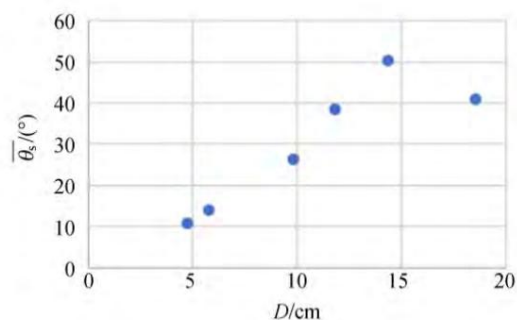
The stronger the resistance stability, the stronger the resilience stability, the comprehensive

The stronger the stability.



(a) at rest (b) pulling off the weight (c) critical release angle

Figure 18 Weight impact (sphere)

Figure 19 $\bar{\gamma}_s$ and \bar{D} relation (sphere)

3.2 Interpretation of stability

Cylinders and spheres are bound to vertical after being disturbed.

Offset in vertical and horizontal directions, pressure generated by flow around the side

The change will give the cylinder the restoring force in the horizontal direction, the impulse of the water column

The change will give the vertical restoring force of the cylinder,

3.2.1 Restoration force in the horizontal direction

Bernoulli's equation applies to the steady flow of an ideal fluid when

When the cylinder is finally in stable suspension, the water on its sides

A flow can be viewed as a steady flow:

$$p + \frac{1}{2} \rho v^2 + \rho gh = C, \quad (10)$$

In formula (10), C is a constant, the highest water column when the cylinder is removed the height is h , then

$$C = \rho gh_0, \quad (11)$$

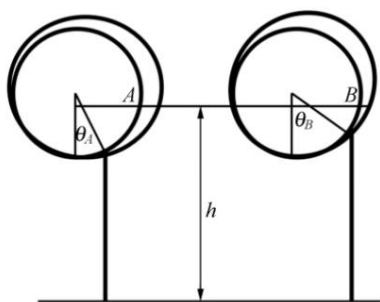
For the same cylinder, when its horizontal offset is different, the

The magnitude of the horizontal restoring force is also different, which can be divided into two categories for discussion:

Figure 20 shows the points at which the water column hits the cylinder at different times different, resulting in different flow around the side surface of the cylinder, (a) Both cases and (b) are not stable cases, from equations (10) and (11) we get:

$$p_A + \frac{1}{2} \rho v_A^2 + \rho gh = \rho gh_0, \quad (12)$$

$$p_B + \frac{1}{2} \rho v_B^2 + \rho gh = \rho gh_0, \quad (13)$$



(a) left (b) right

Figure 20 Horizontal restoring force

The energy loss at the point A and B of the water column mainly includes

Gravitational potential energy loss, viscous drag loss and conversion to impact force

loss, the same as gravitational potential energy loss, viscous drag and transformed impact force

loss and all points A is greater than B, so the residual kinetic energy $E_{KA} <$

E_{KB} , then there are $V_A < V_B$ the point, combining equations (12) and (13), we get

$$p_A > p_B. \quad (14)$$

Consider the overall pressure distribution on the sides of the cylinder combined with the atmosphere

pressure, and finally obtain the pressure gradient force direction to the right, as

$$dF_A = [p_0 - (p_0 - p_A)] dS,$$

$$dF_B = p_0 - (p_0 - p_B) S,$$

Among F_A is the level produced by the pressure distribution for the case of Fig. 20(a)

them, the resilience

$$F_A = \int p_A dS,$$

F_B is the horizontal loop generated by the pressure distribution for the case of Fig. 20(b).

Rejuvenation

$$F_B = \int p_B dS,$$

Combining formula (14), we get:

$$F_A < F_B, \quad (15)$$

F_A and F_B The direction is to the right, to put it figuratively, within a certain range, the bias

The larger the central angle, the more force the cylinder is adsorbed by the water column.

Then consider the component force of the impact force along the horizontal direction, by formula (4),

To get the impact F_1 , the eccentricity angle θ it's time

force change:

$$F_{1x} = 2 \rho g \omega^2 R^4 \cos \theta \sqrt{(h_0 - h) h_0}.$$

component of the impact force along the horizontal direction F_{1x} (for

$$F_{1x} = 2 \rho g \omega^2 R^4 \sin(2\theta) \sqrt{(h_0 - h) h_0}.$$

(reconsider the two cases in Figure 20, for the case of Figure 20(a)

The component force of the impact force along the horizontal direction (acting and restoring force

on the contrary):

$$F_{Ax} = 2 \rho g \omega^2 R^4 \sin(2\theta_A) \sqrt{(h_0 - h_A) h_0},$$

F_{Bx} is the component force of the impact force along the horizontal direction in the case of Fig. 20(b):

$$F_{Bx} = 2 \rho g \omega^2 R^4 \sin(2\theta_B) \sqrt{(h_0 - h_B) h_0}.$$

The angle measured by the experiment $\theta_A < \theta_B$, and because

θ_B , get:

$$F_{Ax} > F_{Bx}, \quad (17)$$

Combining equations (15) and (16) to get

$$F_{Ax} - F_{Bx} < 0 < F_{Bx} - F_{Ax} = F_{Bx} - F_{Ax}. \quad (16)$$

In Fig. 20(a), the eccentric angle is large, and the cylinder receives the horizontal

The restoring force is to the left, and the cylinder in Fig. 20(b) is subjected to a horizontal return to the right.

The complex force, from the zero-point existence theorem, must exist to make the cylinder just reach

to the point of equilibrium, free from restoring forces, i.e. $\theta_A = \theta_B$, Make

$$F_{Ax} - F_{Bx} = 0.$$

3.2.2 Restoring force in the vertical direction

The impact force is obtained from equation (4) F_1 Component along the vertical direction

$$F_{1y} = 2 \rho g \omega^2 R^4 \cos^2 \theta \sqrt{(h_0 - h) h_0}.$$

h (represents the real-time suspension height, which is a time variable. F_{Ay} for Figure 21

The component force of the impact force along the vertical direction in the case of (a):

$$F_{Ay} = 2 \rho g \omega^2 R^4 \cos^2 \theta_A \sqrt{(h_0 - h_A) h_0}.$$

F_{By} is the component force of the impact force along the vertical direction in the case of Fig. 21(b)

$$F_{By} = 2 \rho g \omega^2 R^4 \cos^2 \theta_B \sqrt{(h_0 - h_B) h_0}.$$

Obviously $F_{Ay} < F_{By}$ The vertical restoring force in Fig. 21(a) is F_{Ay} back,

the direction is down:

$$F_{Ay} - G < 0;$$

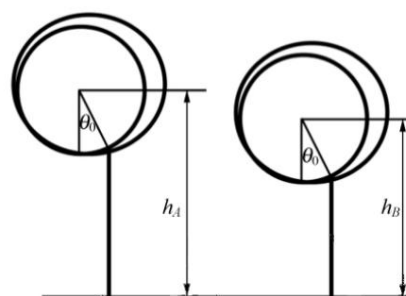
The vertical restoring force in Fig. 21(b) is F_{By} back, direction up:

$$F_{By} - G > 0,$$

From the zero-point existence theorem, there must exist such that the cylinder is just flat

The point of equilibrium, not subject to restoring force, i.e. $\theta_A = \theta_B$, so that

$$F_{Ay} - F_{By} = 0.$$



(a) down (b) up

Figure 21 Vertical restoring force

3.2.3 The lowest point of potential energy

The lowest point of potential energy (θ), the physical meaning of which is that the cylinder is

The point to which the disturbance tends. Numerical simulation using iterative heuristics method to obtain the suspension height and rotational speed of the cylinder when it is stable. for The perturbed cylinder has a time-varying water velocity field around it. , so the exact location of the lowest point of potential energy cannot be obtained. but Does not affect the theoretical existence of the lowest point of potential energy, the existence of this point is very important to the circle It provides a reasonable explanation that the cylinder can return to the stable point after being disturbed.

As shown in Figure 22, for the resistance stability and recovery force stability The qualitative consistency can also be explained in terms of potential energy, since the potential the existence of the $\dot{\psi}$ minimum (), and the potential energy curve is continuous, As a result, there is a valley area in the potential energy curve, and the depth and potential energy of the valley are the smallest. $U(\psi)$ value) is negatively correlated, the smaller the potential energy minimum value in suspension, the lower the deeper. After the object falls, its potential energy is the potential energy of the external environment, namely Falling from the peak to the outside of the flat potential energy curve.

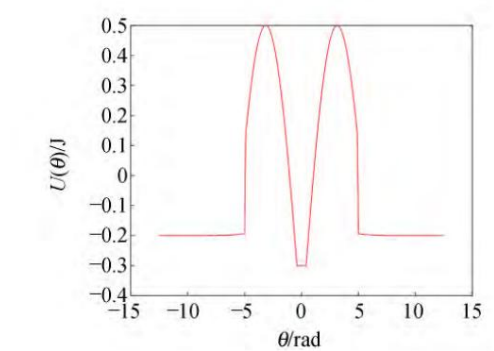


Figure 22 Potential energy curve (qualitative)

For the convenience of understanding, it can be compared to a small ball at the bottom of the valley, which resists The experiment of force stability is to continuously increase the deflection angle of the jet, which is equivalent to The lowest point of potential energy keeps getting bigger, that is, the bottom of the valley rises slowly, as shown in Figure 23 As shown, when the bottom of the valley rises above the peak, the suspended matter falls to the outside in the world environment.

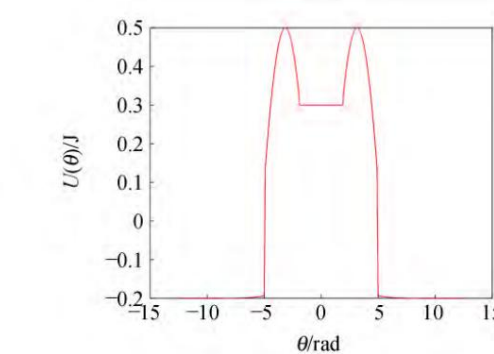


Figure 23 Lifting of the lowest point of potential energy

The restoring force stability experiment is to hit the ball, and the whole The suspension system is unchanged, so the depth of the bottom of the valley is unchanged, but Slowly pull the ball from the bottom of the valley to the top of the peak, after the ball reaches the top, That is, the suspended matter falls into the external environment. So the initial depth of the valley bottom The deeper the degree, the resistance stability and recovery force stability of the suspension are larger, demonstrating that resistance stability and resilience stability have There is consistency.

4 Conclusion

The velocity field of the flow around the cylinder is determined, and the Theoretical suspension height and theoretical rotational speed, the degree of agreement between experiment and theory good. discussed the stability of suspended objects, studied the influence of spheres The factors of the stability of the body and the cylinder, the experimental results show that the rotation speed is related to thickness, diameter, diameter. Positive correlation, suspension height and thickness I D Inversely correlated, for foam cylinders, resistance and recovery The complex force stability is consistent, I = 3.02 cm, D = and its stability is the strongest at 11.81 cm. For foam spheres, the The stability of resistance and recovery force is also consistent, the strongest D = at 14.37 cm, and the sphere with the same diameter recovers more than the cylinder Strong stability.

references:

[1] Zhang Yuanyuan, Duan Tianying, Chen Shuming, et al. Liquid suspension passive rod Control system research and design [J]. Instrument user, 2020, 27 (5): 1-4.

[2] Yuan Haoran, Kuang Bo, Liu Pengfei, et al. liquid suspension passive shutdown Test verification of component drop bar analysis program [J]. applied technology, 2019, 46(6): 1-6.

[3] Zhang Mingyuan. Fluid Mechanics [M]. Beijing: Higher Education Press, 2010: 1-230.

[4] Hou Guoxiang. Fluid Mechanics [M]. Beijing: Machinery Industry Press, 2015: 1-225.

[5] Wang Hongwei. Fluid mechanics as I understand it [M]. Beijing: National Defense Industry Industry Press, 2014: 123-186.

[6] Zhou Xin, Zhang Wei, Cui Hong. Resilience and resilience of ecosystems stabilized Sex [J]. Biology Teaching, 2014, 39(4): 4-5.

[7] Li Xuan, Li Dashuai, Wang Junjie, etc. Inclined Variable Section Management Ideal Fluid Construction of jet model [J]. Physical Experiments, 2018, 38(5): 52- 55.

(Continue to page 58)

